Enhanced fourth-power algorithm for phase estimation with frequency separation in direct-detection optical OFDM systems

Min Kong (孔 敏)[1], Jiangnan Xiao (肖江南)[1], Ze Dong (董 泽)[1,2], Liuqingqing Yang (杨柳青青)[1], Lin Chen (陈 林)[1*], and Jianjun Yu (余建军)[1,2,3]

[1]*Key Laboratory for Micro-/Nano-Optoelectronic, Devices of Ministry of Education, Department of Information Science and Engineering, Hunan University, Changsha 410082, China*

[2]*ZTE USA, Morristown, NJ 07960, USA*

[3]*Fudan University, Shanghai 200433, China*

[*]*Corresponding author: liliuchen12@vip.163.com*

Received December 17, 2012; accepted March 28, 2013; posted online May 31, 2013

The optical orthogonal frequency division multiplexing (OFDM) signal is affected by impairments introduced by electrical filters and optical chromatic dispersion. An enhanced fourth-power algorithm for phase estimation with frequency separation is used to estimate and compensate the phase rotation of OFDM subcarriers. The performance of the proposed phase estimation algorithm is evaluated on a 4-Gb/s OFDM signal at different frequencies. Experimental results using the proposed algorithm show a 1.8-dB received power sensitivity improvement at a bit error rate of 1×10^{-4} after a 100-km standard single-mode fiber transmission, compared with the conventional technique.

OCIS codes: 060.0060, 060.2330, 060.5060.
doi: 10.3788/COL201311.060602.

Optical orthogonal frequency division multiplexing (OFDM) has been proposed as a promising solution to significantly improve transmission performance because of its high-spectral efficiency and superior resilience against fiber chromatic dispersion (CD)[1,2]. However, OFDM signal suffers severely from phase noise due to its long symbol duration[3]. In optical OFDM systems, the phase noise results from the walk-off caused by CD, leading to deteriorated phase coherence during detection. Severe phase noise will lead to stronger inter-carrier interference and phase rotation, which will always dominate the system performance[4].

To date, based on different optical receiver structures, optical OFDM systems can be categorized as either direct-detection optical OFDM (DDO-OFDM) or coherent optical OFDM (CO-OFDM)[5−7]. Relative to CO-OFDM, the simple structure of direct-detection (DD) system can be advantageous for the development of low-cost systems. In CO-OFDM, phase incoherency between the laser source and the remote local oscillator results in phase noise[8−10]. However, in the case of DDO-OFDM, the carrier and the sideband would gradually walk off with increased transmission length, eventually resulting in loss of phase coherency[3]. Numerous approaches have been proposed to estimate phase rotation, either jointly or individually, in wireless communication systems or coherent optical communications, such as pilot subcarriers and RF-pilot[8,11,12]. However, few proposals are put forward to overcome performance degradation caused by phase noise in DDO-OFDM systems. Peng *et al.*[13] applied a simple Wiener filter to adaptively estimate the statistically unknown phase noise, which inevitably increased the hardware complexity and greatly reduced the flexibility for real-time systems. Liang *et al.*[14] proposed an optical OFDM phase shift and compensation method in the frequency domain by sending training sequences and analyzing phase shifts in the DDO-OFDM signals. However, high-phase estimation accuracy under experimental conditions could not be obtained.

In this letter, we theoretically and experimentally investigate the effects of impairments on optical OFDM signal at different frequencies. Based on the frequency characteristics of the OFDM signal, an enhanced fourth-power algorithm for phase estimation (FP-PE) with frequency separation is presented[12,15], which is used to estimate and compensate for the phase rotation of DDO-OFDM subcarriers caused by frequency selective fading, subcarrier-to-subcarrier mixing interference, and other nonlinear effects[16,17]. The experimental results demonstrate that a 4-Gb/s DDO-OFDM signal combined with the proposed phase estimation algorithm has superior phase noise tolerance compared with conventional techniques without phase estimation.

Derivation of the mathematical model for the DDO-OFDM system is described below[18]. A steady and monochromatically distributed feedback (DFB) laser is used as the light source and can be simplified in the time domain as

$$C(t) = A_{\mathrm{o}} \cos\left(\omega_{\mathrm{o}} t\right), \tag{1}$$

where A_{o} and ω_{o} represent the amplitude and frequency of the optical carrier, respectively. The OFDM signal in the time domain can be defined as

$$S\left(t\right) = \sum_{k=1}^{N} \left(a_k \cos k\Omega t + b_k \sin k\Omega t\right), \tag{2}$$

where N denotes the number of subcarriers in an OFDM symbol, t denotes the time, Ω is the first subcarrier frequency, $k\Omega$ is the frequency of the kth subcarrier, and

a_k and b_k represent the complex symbols of the in-phase (I) and quadrature (Q) components for the kth subcarrier, respectively. The electrical OFDM signal output is directly modulated on the optical carrier with double side band (DSB) modulation by an intensity modulator (IM). After digital-to-analog conversion (DAC) and reconstruction filtering, signal degradation occurs during digital signal processing (DSP). The signal after OFDM modulation can be written as

$$E_{\text{out}}(t) = A_{\text{o}}\cos(\omega_{\text{o}}t)\left[1+\gamma\sum_{k=1}^{N}(a_k\cos k\Omega t + b_k\sin k\Omega t)\right], \quad (3)$$

where γ denotes the optical modulation index in the IM linear range.

The optical OFDM signal being transmitted over a fiber is mainly affected by the fiber chromatic dispersion and polarization mode dispersion, wherein the impairments lead to frequency shift, phase shift, and amplitude attenuation[17]. After transmission over a z-km length fiber with the propagation $\beta(\omega)$ and the amplitude attenuation $\text{Att}(z)$, the optical OFDM signal at the receiver can be rewritten as

$$E_{\text{out}}(t) = A_{\text{o}}\gamma\text{Att}(z)\sum_{k=1}^{N}\cos\Big(\omega_{\text{o}}t-\frac{\beta_1+\beta_2}{2}z\Big)\times B_k + A_{\text{oAtt}}(z)\cos(\omega_{\text{o}}t-\beta_3 z), \quad (4)$$

where

$$B_k = a_k\cos\Big(k\Omega t-\frac{\beta_1-\beta_2}{2}z\Big) + b_k\sin\Big(k\Omega t-\frac{\beta_1-\beta_2}{2}z\Big),$$
$$\beta_1=\beta(\omega_o+k\Omega),\beta_2=\beta(\omega_o-k\Omega),\beta_3=\beta(\omega_o).$$

The square-law photon detector is employed to obtain the optical-to-electrical (O/E) conversion. The unfiltered photon electrical current can be expressed as

$$I=\mu|E_{\text{out}}(t)|^2 = \left[A_{\text{o}}\gamma\text{Att}(z)\sum_{k=1}^{N}\cos\Big(\omega_{\text{o}}t-\frac{\beta_1+\beta_2}{2}z\Big)\times B_k\right]^2 + 2\gamma A_{\text{o}}^2\text{Att}^2(z)\cos(\omega_{\text{o}}t-\beta_3 z)\times\left[\sum_{k=1}^{N}\cos\Big(\omega_{\text{o}}t-\frac{\beta_1+\beta_2}{2}z\Big)\times B_k\right] + A_{\text{o}}^2\text{Att}^2(z)\cos^2(\omega_{\text{o}}t-\beta_3 z). \quad (5)$$

Given that the square-law photon detector at a certain bandwidth is insensitive to high-frequency optical OFDM signal, optical carrier-containing components can be considered as DC components. The OFDM signal after the optical band-pass filter (OBPF) can then be expressed as

$$I=\gamma^2A_{\text{o}}^2\text{Att}^2(z)\Big[\sum_{k=1}^{N}\cos\Big(\omega_{\text{o}}t-\frac{\beta_1+\beta_2}{2}z\Big)\times B_k\Big]^2 + \gamma A_{\text{o}}^2\text{Att}^2(z)\Big[\sum_{k=1}^{N}\cos\Big(2\omega_{\text{o}}t-\frac{\beta_1+\beta_2+2\beta_3}{2}z\Big)\times B_k + \sum_{k=1}^{N}\cos\Big(\frac{\beta_1+\beta_2-2\beta_3}{2}z\Big)\times B_k\Big] + A_{\text{o}}^2\text{Att}^2(z)\cos^2(\omega_o t-\beta_3 z), \quad (6)$$

$$I=\gamma^2A_{\text{o}}^2\text{Att}^2(z)\left(\sum_{k=1}^{N}B_k\right)^2+\gamma A_{\text{o}}^2\text{Att}^2(z)\cdot\left[\sum_{k=1}^{N}B_k+\sum_{k=1}^{N}\cos\Big(\frac{\beta_1+\beta_2-2\beta_3}{2}z\Big)\times B_k\right]+A_{\text{o}}^2\text{Att}^2(z) = \gamma A_{\text{o}}^2\text{Att}^2(z)\cdot\left[\sum_{k=1}^{N}\cos\Big(\frac{\beta_1+\beta_2-2\beta_3}{2}z\Big)\times B_k\right] \text{-----OFDM} + \gamma^2A_{\text{o}}^2\text{Att}^2(z)\left(\sum_{k=1}^{N}B_k\right)^2\text{----------SSMI} + A_{\text{o}}^2\text{Att}^2(z)\Big(\gamma\sum_{k=1}^{N}B_k+1\Big)\text{----------DC}. \quad (7)$$

From the equation above, the output signal contains three parts: OFDM signal, subcarrier-to-subcarrier mixing interference (SSMI), and DC. The signal is affected by impairments in the DDO-OFDM system after passing through electrical filters and a span of fiber transmission. The impairments mainly have three forms: 1) frequency selective fading (FF) due to electrical filters and DAC/ADC conversion during electrical signal processing; 2) SSMI generated by the beating between OFDM subcarriers; 3) optical CD, polarization-mode dispersion, and FF due to symbol delay caused by the dispersion[18–20]. Among the three impairments, the third is the most important factor.

The principle of the optical OFDM system and the OFDM signal impairments at different locations are shown in Fig. 1. Figures 1(ii), (iii), (iv), and (v) represent FF, SSMI, OFDM signal affected by phase shifting, and OFDM signal after photodiode (PD) and ADC conversion, respectively. From the diagram, the OFDM signals undergo a phase and amplitude distortion. In addition, the impairments have different influences on the DDO-OFDM signal at different frequencies. The effect of impairments on high-frequency OFDM signals is greater than that on low-frequency signals because high-frequency OFDM subcarriers are greatly influenced by the FF and non-ideal spectrum characteristics of electronic devices.

The principle diagram of the FP-PE is shown in Fig. 2[9,12,21].

The received signal comprises data-modulated signal

and phase noise, and can be written in normalized form as

$$r(k) = d(k)\exp[\mathrm{j}\theta(k)], \tag{8}$$

where $\theta(k) = \theta_s(k) + \Delta\psi$, $r(k)$ is the received signal, $d(k)$ denotes the amplitude of the received signal, and $\theta(k)$ denotes the phase of received signal, which is influenced by the modulated phase $\theta_s(k)$ and the phase rotation $\Delta\psi$ caused by phase noise. $\Delta\psi$ is estimated using the following procedures: first, the modulated phase $\theta_s(k)$ should be adjusted to $\theta'_s(k)$, such that four times of $\theta'_s(k)$ can be cancelled on the basis of 2π phase periodicity. The phase transformation can be expressed as

$$\begin{cases} \theta_s(k) \subset \left\{\dfrac{\pi}{4}, \dfrac{3\pi}{4}, \dfrac{5\pi}{4}, \dfrac{7\pi}{4}\right\} \\ \theta'_s(k) \subset \left\{\dfrac{\pi}{2}, \pi, \dfrac{3\pi}{2}, 2\pi\right\} \\ 4 \times \theta'_s(k) \subset \{2\pi, 4\pi, 6\pi, 8\pi\} \end{cases}. \tag{9}$$

Afterward, certain continuous symbols are divided into the same group and raised to the Mth power. For QPSK modulation, the value of M is 4. The received signal can be expressed as

$$s(k) = [r(k)]^M = [d(k)]^M \exp[4 \times \theta'_s(k) + 4 \times \Delta\psi]. \tag{10}$$

After the continuous symbols are summated, the next step is to average the real and imaginary vectors of the summation and subtract $\overline{\theta_n(k)}$ from its average phase. Finally, the estimated phase $\overline{\Delta'\psi}$ can be obtained by dividing the average phase with M, wherein

$$\begin{cases} \overline{\theta_n(k)} = \overline{4\Delta'\psi} \\ \theta_0(k) = \frac{1}{M}\overline{\theta_n(k)} = \overline{\Delta'\psi} \end{cases}. \tag{11}$$

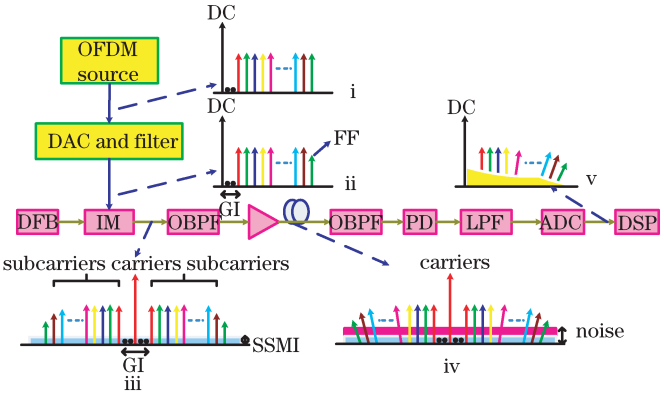

Fig. 1. Principle of optical OFDM and signal impairments at different locations. (i) After OFDM modulation; (ii) after DAC and filter; (iii) after optical IM; (iv) after fiber transmission; (v) after O/E detection and ADC. LPF: low-pass filter, GI: guard intervals.

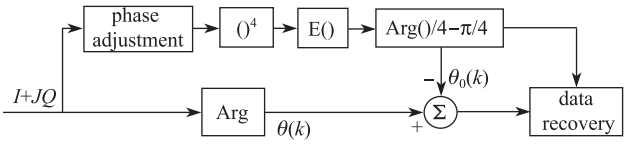

Fig. 2. FP-PE algorithm.

A phase adjustment before the phase estimation algorithm occurs; thus, $\pi/4$ must be subtracted from the estimated phase $\theta_0(k)$ to restore the signal point to the previous position. The final accurate estimated phase is shared by this group of continuous symbols, in which each input symbol achieves the output phase after subtracting the final phase estimated from the received signal phase $\theta(k)$.

In particular, from the average phase $\overline{\theta_n(k)}$, the superiority of the phase estimation algorithm with separated compensation in accordance to frequency can be clearly observed. The impairments have different effects on the DDO-OFDM signal at various frequencies, and a phase estimation algorithm with frequency separation can obtain higher phase estimation accuracy in the aforementioned system.

Figure 3 shows the enhanced FP-PE with frequency separation. At the receiver, the received electrical OFDM signal should be normalized and separated according to the OFDM subcarrier frequency. The length of the frame is L and the number of subcarriers in each frame is N. Firstly, the subcarriers on all of the frames are divided into N large groups according to their frequencies. Subcarriers with similar frequencies are classified under the same group. Secondly, subcarriers with similar frequencies are further divided into smaller L/t subgroups, and the number of subcarriers in each subgroup is t. Thirdly, the FP-PE algorithm is adopted on the subcarriers of each subgroup to estimate and compensate the common phase rotation of the subgroups. When the common phase rotation of all the subgroups at the first large group are estimated and compensated, the next step is to estimate and compensate the phase rotation of other large groups in a similar manner. Finally, the data signal should return to the previous position so that the original signal can be demodulated correctly.

A particular qualitative conclusion about the chosen groups can be drawn. The block length t of each subgroup must not be extremely large or small; a moderate value is better. The larger the designed value of t is, the better the effect of averaging phase noise will be. However, if the value of t is too large, the premise that the phase rotation of continuous symbols can be regarded as similar will not be hold true; thus, the phase estimation accuracy will be affected. Moreover, although the enhanced algorithm increases the computation complexity of the system to a certain extent, the grouped structure of this proposed algorithm provides a possibility of parallel processing for multiple grouped blocks, thereby further improving the system efficiency.

Figure 4 shows the DDO-OFDM transmission system with OFDM signal generation, E/O modulation, optical transmission, O/E demodulation, and received OFDM signal processing. OFDM modulation is implemented using MATLAB with off-line programming. At the transmitter, the pseudorandom binary sequence bits are subjected to OFDM modulation, including serial-to-parallel conversion, MAP (QPSK modulation), inverse fast Fourier transform, parallel-to-serial conversion, and circle prefix addition. The discrete digital signal is converted to a continuous electrical signal by an arbitrary waveform generator (AWG), which serves as the digital/analog converter. The electrical OFDM signal is

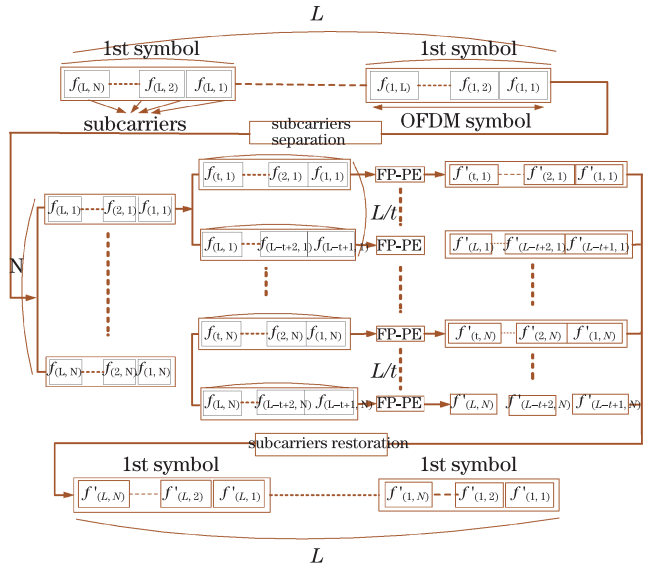

Fig. 3. Diagram of the enhanced FP-PE algorithm with frequency separation.

modulated directly on an optical carrier with DSB modulation over SSMF. At the receiver, the optical OFDM signal is converted to an electrical OFDM signal after detection by a PD. The received electrical signal is then sampled by a real-time oscilloscope and processed off-line for demodulation, which is the inverse transformation of the transmitter. In particular, after the transformation of the fast Fourier transform (FFT), the proposed phase estimation algorithm is adopted in the received symbols, and is used to mitigate the impairments of the DDO-OFDM system with phase noise. Notably, no known symbols, such as training sequences and pilot subcarriers, are inserted at the transmitter for channel estimation.

The experimental setup for the DDO-OFDM system is shown in Fig. 5. In this experiment, the length of frame is 2000 and the number of subcarriers in each frame is 32, with a cyclic prefix of 4 samples in every OFDM frame. QPSK is employed for signal modulation. OFDM modulation of the digital data is implemented off-line using MATLAB. The required analog electrical signal to be transmitted is generated by an AWG, with a sample rate of 10-GS/s signal. The 12.5-dBm output power light-wave is generated from a commercial DFB laser at 1 565.48 nm and modulated by an analog electrical OFDM signal to generate the optical OFDM signal through an optical IM with a bias voltage of 1.66 V. The DFB laser linewidth is less than 2 MHz. The optical OFDM signal is amplified to 4 dBm by EDFA1 prior to transmission. After transmission over a 100-km SSMF-28, the optical signal is pre-amplified by EDFA2 to 4 dBm and then filtered through a 1-nm bandwidth OBPF. At the receiver, the optical OFDM signal undergoes O/E conversion using a commercial optical receiver with a 3-dB bandwidth of 10 GHz. The power of the detected optical signal can be adjusted by a tunable attenuator. The converted electrical OFDM signal is sampled using the Tektronix real-time oscilloscope at 3-dB bandwidth of 8 GHz and stored for processing off-line in MATLAB[1,22].

The electrical spectra of a 4-Gb/s optical OFDM signal sampled by a real-time oscilloscope are indicated in Fig. 5. The blue spectrum represents the electrical spectrum of the OFDM signal before transmission, whereas the black spectrum represents the electrical spectrum after transmission. The OFDM signal is modified after passing through electrical filters and fiber transmission. The influence on high-frequency OFDM signals is greater than that on low-frequency signals. This result proves that OFDM signal is affected by optical dispersion and that the effect on optical OFDM signal is relevant to the subcarrier frequency. Therefore, the optical OFDM signal phase rotation should be estimated and compensated separately according to the frequency.

We perform a comparative research on the received DDO-OFDM signal with and without the proposed phase estimation algorithm. A comparative analysis of the performances of high-frequency, intermediate-frequency, and low-frequency OFDM signals is also performed. The subcarriers are divided into three groups: subcarrier index varying from 1 to 5 represent high-frequency OFDM signal, subcarrier index varying from 6 to 10 represent intermediate-frequency OFDM signal, and subcarrier index varying from 11 to 16 represent low-frequency OFDM signal.

Figure 6 shows the errors of OFDM signal at different frequencies. The received signal constellations at high, intermediate, and low OFDM signal frequencies when the received optical power is –27 dBm are also recorded. OFDM signal errors at different frequencies without the proposed phase estimation algorithm are shown in Fig. 6(a), whereas the OFDM signal errors at different frequencies with the proposed phase estimation algorithm are shown in Fig. 6(b). From Fig. 6, subcarriers at different frequencies can be observed to suffer from phase

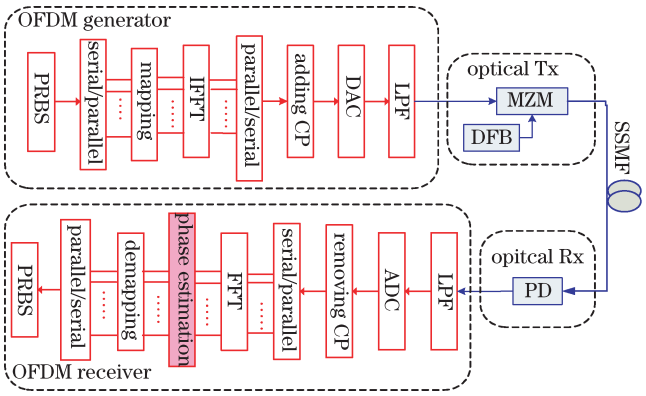

Fig. 4. Principle of DDO-OFDM transmission system. Tx: transmitter, Rx: receiver.

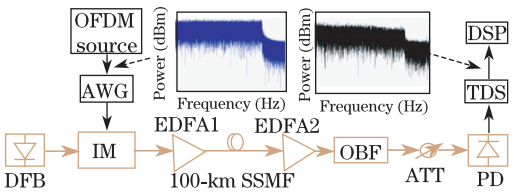

Fig. 5. Experimental setup of DDO-OFDM transmission system. The electrical spectra of OFDM signals are indicated. EDFA: erbium-doped fiber amplifier, OBF: optical band-pass filter, ATT: attenuator, TDS: real-time storage oscilloscope.

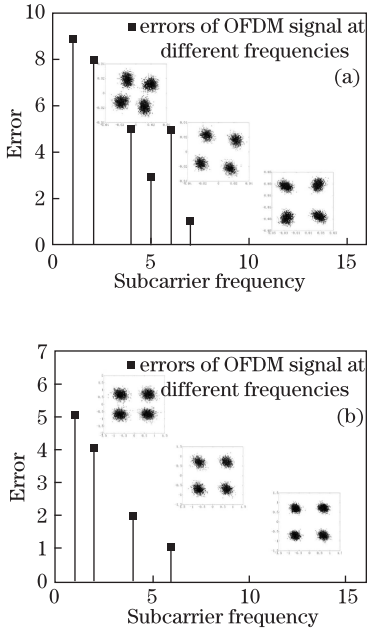

Fig. 6. Errors of the OFDM signal at different frequencies. The received signal constellations at high, intermediate, and low OFDM signal frequencies when the received optical power is -27 dBm are also indicated. (a) Without the proposed phase estimation algorithm; (b) with the proposed phase estimation algorithm.

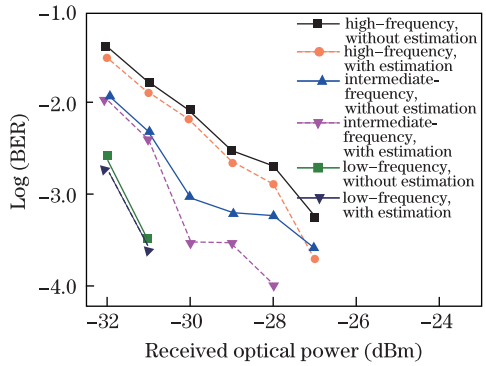

Fig. 7. Measured BER curves of high, intermediate, and low OFDM signal frequencies against different received powers.

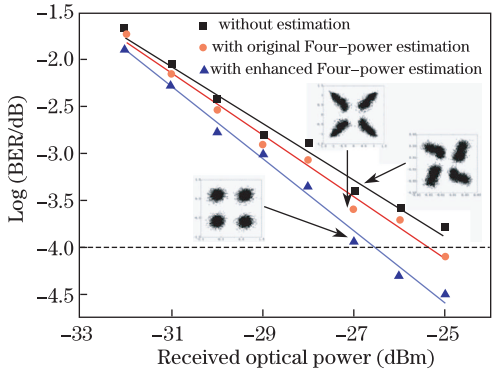

Fig. 8. Curves of the measured OFDM signal BER against different receiving optical powers. The received signal constellations when the receiving optical power is –27 dBm are indicated.

rotation at different levels, with the rotary levels of high- and intermediate-frequency signals being worse than those of the low-frequency signals. By using the proposed phase estimation algorithm, the errors of OFDM subcarriers at different frequencies are greatly reduced. The received signal constellations of the three classifications have become convergent, in which the phase rotation of subcarriers has been basically corrected.

The bit-error rate (BER) performance of the DDO-OFDM system with and without the proposed phase estimation algorithm is analyzed by monitoring the reception sensitivity. Figure 7 shows the measured BER performance at high, intermediate, and low OFDM signal frequencies against different received powers. The solid lines represent the measured BER performance without the proposed phase estimation algorithm, and the dotted lines represent the measured BER performance with the proposed phase estimation algorithm. The BER performance of the OFDM signal varies at different frequencies. Furthermore, the BER performance of the OFDM signal at high and intermediate frequencies is worse compared with that at low frequency. By using the proposed phase estimation algorithm, the BER performance of OFDM signal has been improved.

Curves of the measured BER of the OFDM signal against different received optical powers are shown in Fig. 8. The received signal constellations when the receiving optical power is –27 dBm are also recorded. The BER performance of the OFDM system is improved after adopting the phase estimation algorithm, in which the enhanced fourth-power algorithm is observed to be superior to the original fourth-power algorithm without frequency separation. The required receiving optical power for the OFDM signal without any phase estimation, with the original four-power estimation, and with the enhanced four-power estimation algorithm at a BER of 1×10^{-4} are –24.8, –25.4, and –26.6 dBm, respectively. This result indicates a 1.8-dB improvement in the receiving power sensitivity at a BER of 1×10^{-4} after a 100-km SSMF transmission by employing the proposed phase estimation algorithm.

In conclusion, an enhanced FP-PE with separated compensation in accordance to frequency is proposed. The experimental result shows that the proposed phase estimation algorithm can obtain better phase estimation accuracy and higher receiver sensitivity. For the 4-Gb/s OFDM signal, a 1.8-dB receiving power sensitivity improvement is achieved at a BER of 1×10^{-4} after 100-km SSMF transmission by employing the proposed phase estimation algorithm. Our theoretical and experimental results prove that the algorithm is efficient in estimating and compensating for the phase rotation of the optical OFDM signal at all frequency bands. Although the proposed algorithm increases the computational complexity of the system to a certain extent, this algorithm is also advantageous in the spectral utilization of DDO-OFDM systems.

This work was supported by the National Natural Science Foundation of China (No. 60977049), the National "863" Program of China (No. 2011AA010203), and the Hunan Provincial Natural Science Foundation (No. 12JJ3070).

References

1. X. Gu, H. Chen, Q. Tang, M. Chen, and S. Xie, Chin. Opt. Lett. **10,** 020601 (2012).
2. A. Jean, J. Lightwave Technol. **27,** 189 (2009).
3. W. R. Peng, IEEE Photon. Technol. Lett. **28,** 2526 (2010).
4. X. Liu, Y. Qiao and Y. Ji, Chin. Opt. Lett. **9,** 030602 (2011).
5. L. Chen, Z. Cao, Z. Dong, and J. Yu, Chinese J. Lasers (in Chinese) **36,** 554 (2009).
6. Z. Cao, J. Yu, J. Xiao, and L. Chen, J. Lightwave Technol. **28,** 2423 (2010).
7. Y. Xu, Y. Qiao and Y. Ji, Chin. Opt. Lett. **10,** 110601 (2012).
8. W. Shieh, IEEE Photon. Technol. Lett. **20,** 605 (2008).
9. S. J. Savory, Opt. Express **16,** 804 (2008).
10. E. Mohammad, M. Pasandi, and D. Plant, IEEE Photon. Technol. Lett. **23,** 1594 (2011).
11. M. G. Taylor, J. Lightwave Technol. **27,** 901 (2009).
12. A. Leven, N. Kaneda, U.-V. Koc, and Y.-K. Chen, IEEE Photon. Technol. Lett. **19,** 336 (2007).
13. W. R. Peng, I. Morita, and H. Tanaka, in *Proceedings of ECOC 2010* Tu.3.C.3 (2010).
14. M. Liang, J. He, and Q. Ma, Opt. Commun. Technol. **2,** 45 (2011).
15. Y. Gao, J. Yu, J. Xiao, and L. Chen, J. Lightwave Technol. **18,** 2423 (2010).
16. W. R. Peng, I. Morita, and H. Tanaka, J. Lightwave Technol. **30,** 2025 (2012).
17. B. C. Schmidt, A. J. Lowery, and J. Armstrong, J. Lightwave Technol. **27,** 2792 (2009).
18. Y. Gao, J. Yu, J. Xiao, Z. Cao, F. Li, and L. Chen, J. Lightwave Technol. **29,** 2138 (2011).
19. Z. Cao, J. Yu, W. Wang, L. Chen, and Z. Dong, IEEE Photon. Technol. Lett. **22,** 736 (2010).
20. H. Yi, E. Viterbo, and A. Lowery, in *Proceedings of ECOC 2011* Th.11.B.2 (2011).
21. X. Liu, H. Liang, B. Dai, and B. Lan, Chin. Opt. Lett. **10,** S10609 (2012).
22. L. Li, Y. Qiao, and Y. Ji, Chin. Opt. Lett. **9,** 060604 (2011).